Magazine of Civil Engineering

ISSN 2071–0305

journal homepage: http://engstroy.spbstu.ru/

DOI: 10.18720/MCE.91.6

The fine high-calcium fly ash as the basis of composite cementing material

O.M. Sharonova*, V.V. Yumashev, L.A. Solovyov, A.G. Anshits
Federal Research Center «Krasnoyarsk Science Center of the Siberian Branch of the Russian Academy of Sciences», Krasnoyarsk, Russia
** E–mail: sharon05@yandex.ru*

Keywords: high-calcium fly ash, cementitious materials, superplasticizer, hydration, compressive strength, calcium compounds, X-ray diffraction

Abstract. The high-calcium fly ashes (HCFA) of Krasnoyarsk TPP-2, Russia were studied. The HCFA were selected from each of the 4 fields of the electrostatic precipitator. It was determined that the size distribution, chemical and quantitative phase composition vary significantly from 1st to 4th EF field. The fine high-calcium fly ash (d_{90} < 10 microns) selected from the fourth field of electrostatic precipitator was the source for high strength specimens. In the composition with a superplasticizer at a water:binder ratio of W/B = 0.25 the specimens were made and then cured from 1 to 120 days, with their compressive strength increasing from 17 to 72 MPa. The strength of these specimens is comparable to the strength of specimens based on Portland cement PC 42.5 N without superplasticizer. The methods of simultaneous thermal analysis (STA) and quantitative X-ray phase analysis (XRD) were used to study phase transformations of high-calcium fly ash in the process of hydration curing. The major newly formed phases are ettringite $3CaO•Al_2O_3•3CaSO_4•32H_2O$, as well as calcium carboaluminate hydrates $Ca_4Al_2(OH)_{13}(CO_3)0.5•4H_2O$ and $Ca_4Al_2(OH)_{12}CO_3•5H_2O$ with low crystallinity. The new phases can form a wide range of solid solutions by replacing Al^{3+} with Fe^{3+}. The more the curing age was, the more transformations of calcium silicate amorphous substance contribute to form cryptocrystalline calcium hydrosilicates that increased the initial and long-term strength of the material. The phase transformations and strength indicators allow to use fine high-calcium fly ash of coal-fired power plants as an independent cementing material in modern technologies for producing building materials, in particular, in the technology of self-compacting composite concrete (SCC). The proposed alternative to cement contributes to the solution of a complex environmental problem: (1) in the heat power engineering the accumulation of fine ash particles can be lowered with consequent reduction of the pollution of water, soil and atmosphere with thin dust particles, and (2) in the construction materials industry a part of the cement can be replaced by the fine HCFA, that will save energy and natural resources.

1. Introduction

Although the share of alternative energy sources is growing, the contribution of coal-fired power plants to electricity production remains quite high and is about 40 % in the world [1]. Coal fly ashes, a by-product of coal combustion, have a complex composition, and therefore differ in the properties and methods of utilization [2]. Recycling of coal fly ashes is constantly increasing, they are used in cement and concrete production, road base and pavement construction, soil amendment, zeolite synthesis, ceramic industry; as filler in polymer, but the current average utilization rate is don't exceed 25 % in the world [1–4]. High calcium fly ashes have a smaller contribution to ash wastes compared with aluminosilicate fly ashes, but they are more toxic when stored in ash dumps, since they form alkaline solutions with pH 11–13 [3].

The use of coal ash in the construction industry as a substitute for cement and as an active mineral additive to concrete is the most promising trend of their large-scale use [1–7]. The HCFA are composed of crystalline phases with hydraulic activity (lime, aluminates, sulfates, sulfoaluminates, aluminoferrites of calcium), as well as active glass-crystal microspheres, due to the high content of Ca^{2+} cations in the glass [8–12]. For those reasons, in addition to pozzolanic activity, they have independent cementing properties. Usually 25–40 % of Portland cement (PC) is replaced with such ashes [13]. The use of high-calcium fly ash from the combustion of Kansk-Achinsk coal in the production of autoclaved and non-autoclaved aerated concrete, in addition to saving cement, leads to a decrease in shrinkage and an increase in the strength of products [12].The high-volume fly ash concretes where 50–70 % PC was substituted, are of great interest because they bring ecological, economical and technological benefits [2]. It was shown that it is possible to produce the concrete with the strength of 28–32 MPa by 28 days of hardening, with 100 % replacement of PC with HCFA, in composition with recycled glass [14].

The current trend in the energy industry is the modernization of thermal power plants, in order to increase the degree of exhaust gas purification to 99–99.7 %, including ash particles. This aim was achieved at a number of foreign and Russian thermal power plants by improving the operation of electrostatic precipitators or their combination with bag filters [15]. As a result, the capture of the smallest ash particles less than 10 microns in size and, especially, less than 2.5 microns was increased. Micro- and submicron ash particles can be effectively used in modern technologies to produce new materials, in particular, self-compacting concrete (SCC) with the compressive strength from 50 to 100 MPa [16]. The key element of the SCC technology is the use of polymer superplasticizer, which ensures the effective dispersion of fine cementing components in the liquid phase and the formation of a dense and durable microstructure due to close contact and interaction of the newly formed phases with each other and with unreacted components [16, 17].

High calcium fly ashes trapped in different fields of electrostatic precipitators vary dramatically in fractional composition and, to a considerable extent, in chemical and phase composition [9, 18–20]. It was found [9], that the dispersity increases significantly along the gas-dust flow, for example, 90 % of the fly ash particles from the 1st field are less than 40 microns in size; from the 2nd and 3rd fields are less than 12 microns; from the 4th field are less than 8 microns. It was noticed that the content of CaO, SiO_2, and Fe_2O_3 phases decreases from the 1st to the 4th fields of the electrostatic precipitator, while the contents of $CaSO_4$ and glass increase. Thus, HCFA obtained in different fields of the electrostatic precipitator are ash separation products significantly various in composition and, especially, particle size distribution, and, consequently, in their cementing properties. The main regularities to form the composition and properties of HCFA in the fields of electrostatic precipitators are described by the authors [19, 20]. Based on these data, it was proposed to use finely dispersed fly ashes of the last fields of electrostatic precipitators containing a smaller amount of free CaO, as a binder material.

The aim of this work is to study the dispersity and chemical and phase composition of high-calcium fly ashes, selected from each of the 4 fields of the electrostatic precipitator and to determine their cementing properties, which are promising for obtaining high-strength composite materials.

2. Materials and Methods

2.1. Materials

The objects of the study were high-calcium fly ashes (HCFA) from burning of pulverized low-ash (11 %) brown coal grade B2 of the Kansk-Achinsk basin, Russia. The coal was burned at the Krasnoyarsk TPP-2 (Krasnoyarsk, Russia) in boiler units of the BKZ-420 type with liquid slag removal at a temperature of 1400–1500 °C. High-calcium fly ashes (1–4) were selected from each of the 4 fields of electrostatic precipitator in a facility with an ash collection efficiency of ≥98 %. Portland cement PC 42.5N of the Krasnoyarsk cement plant was taken for comparison.

2.2. Methods

The macro component composition (components SiO_2, Al_2O_3, Fe_2O_3, CaO, MgO, SO_3, Na_2O, K_2O, and TiO_2) and the loss on ignition (LOI)) were determined by chemical analysis methods according to National standard GOST 5382–91. The particle size distribution was measured with a Fritsch Analysette 22 MicroTec laser particle analyzer (Germany) using a dry cell. The SEM images for fly ashes were taken with a Hitachi TM-1000 electron microscope (Japan).

X-ray powder diffraction quantitative phase analysis was carried out using the full-profile Rietveld method and the derivative difference minimization approach [21]. The diffractograms were recorded in the reflection geometry on a PANalytical X'Pert PRO diffractometer (Co $K\alpha$ radiation, graphite monochromator, scan range 2θ = 7–100°) equipped with a PIXcel detector. The weight fraction of crystalline and amorphous components was determined by the external standard method with corundum used as the standard. The overall absorption coefficients of the samples were calculated from the total elemental composition according

to the chemical analysis data. This method was successfully applied to determine the quantitative phase composition of high-calcium fly ash middlings [9] and narrow fractions of ferrospheres recovered from fly ashes [22].

The specimens shaped as 20×20×20 mm cubes were manufactured from 100 % of fly ash selected from each of the 3rd and 4th fields of electrostatic precipitator at a water/binder ratio W/B = 0.4. For comparison, the same specimens were made from 100 % Portland cement PC 42.5N taken from the Krasnoyarsk cement plant. For the finest fly ash of the 4th field of the electrostatic precipitator, the specimens were made at W/B = 0.25 with addition of the Melflux 5581F superplasticizer (0.12 wt %).

The concentration of superplasticizer was chosen according to the results of tests for fluidity. The fluidity was measured at 20 °C from the diameter of a spot of binder paste flowing from a tube with an internal diameter of 50 mm and a height of 51 mm according to JASS 15 M103 [23]. The spot diameter (F) was used to calculate the relative flow surface area (G) characterizing the deformability of a mixture by the equation $G = F^2/50^2 - 1$. At W/B = 0.25, acceptable G = 8 was attained at a Melflux concentration of 0.12 %. The specimens were stored above the water layer in the desiccators for 1, 3, 7, 28, 60, 80, and 120 days. The strength tests of specimens were performed on an Instron 3360 tabletop dual-column testing machine (United States) at a return speed of 5 mm/min.

The simultaneous thermal analysis (STA) of hydrated specimens after drying for 2 h at 60 °C was performed on a Netzsch Jupiter STA 449C analyzer (Germany) with a Netzsch Aeolos QMS 403C mass spectrometer (Germany) in lidded Pt–Rh crucibles using a sample portion of 20.0 ± 0.1 mg. The measurement of the mass change (TG, DTG), the heat flux (DSC), and the composition of gaseous products (by Ar^+, O_2^+, CO_2^+, CO^+, H_2O^+, and SO_2^+ molecular ions) was performed in the mode of linear temperature increase at a speed of 10 °C / min within a temperature range of 40–1000 °C, supplying the 20 % O_2 + 80 % Ar gas mixture (total flow rate, 50 cm^3(NTP)/min).

3. Results and Discussions

3.1. Initial fly ashes

The studied high-calcium fly ashes of 1–4 fields of electrostatic precipitator significantly differ from each other by their fineness (Figure 1). About 90 % of particles (d_{90}) of the fly ashes selected from the 1st and 2nd fields of the electrostatic precipitator are less than 40 microns, and 50 % of particles (d_{50}) are less than 13 microns. The fly ashes of the 3rd and, especially, the 4th field of electrostatic precipitator have a higher dispersity, the value d_{90} of which is about 30 and 10 microns, and d_{50} is about 9 and 4 microns, respectively. The particle size distribution for the PC 42.5 N (Figure 1) is somewhat shifted towards larger particles, the values of d_{90} and d_{50} are 55 and 20 microns, respectively. At the same time, the content of particles less than 10 microns in cement is close to the fly ashes of the 1st and 2nd fields of the electrostatic precipitator.

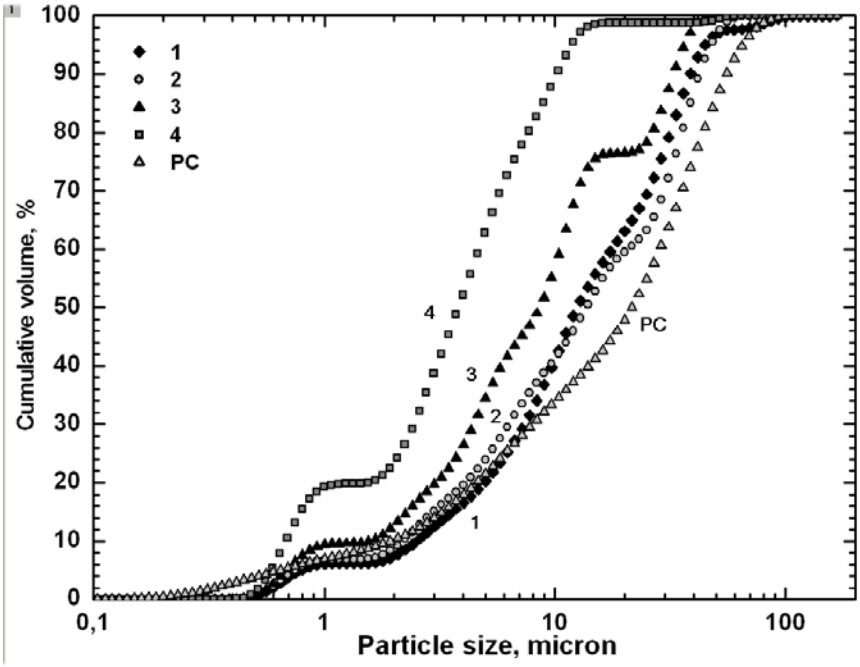

Figure 1. Particle size distribution for HCFA selected from 1–4 fields of the electrostatic precipitator (1–4), and for Portland cement 42.5 N (PC).

The general view of the fly ashes taken from the 1st and 4th fields of the electrostatic precipitator is shown in Figure 2, from which it follows that the fly ashes consist of mainly microspheres with the different size and morphology. The studied high-calcium fly ashes were formed in a boiler with liquid slag removal at a temperature of 1400–1500 °C, which led to the melting of the ash substance and the formation of melt drops in the gas-air flow, and during cooling, microspherical particles [11].

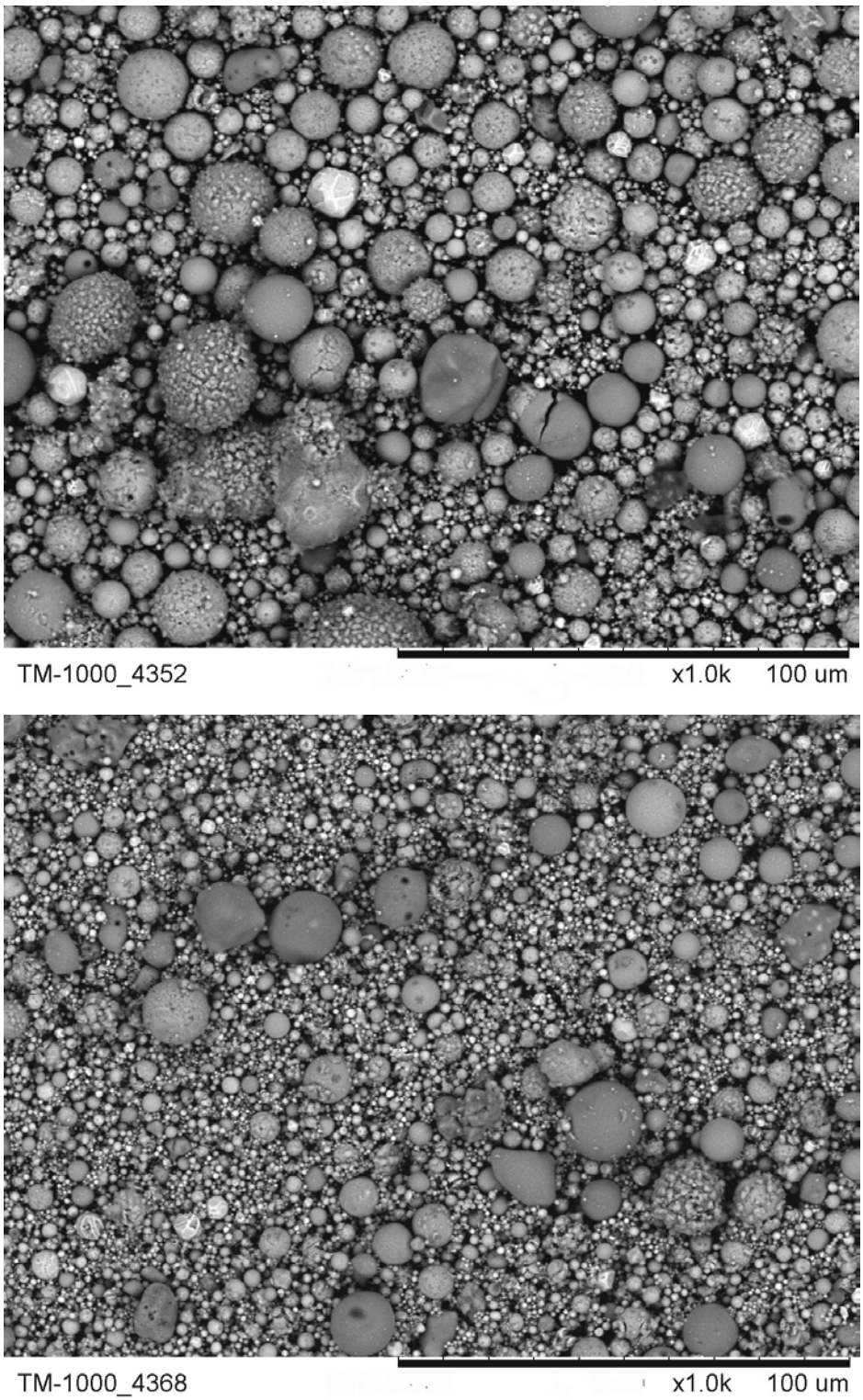

Figure 2. SEM images for HCFA selected from 1st (top) and 4th (bottom) fields of the electrostatic precipitator.

The chemical composition of fly ashes *1–4* (Table 1) is presented by predominant CaO (40–46 wt %), rather plentiful SiO_2 (21–28 wt %), and a much lower content of other macro components (wt %): Al_2O_3 (4–7); Fe_2O_3 (12–14); MgO (8–10) and SO_3 (2–4). The composition of fly ashes 1–4 is close to PC [22, 23] by the content of SiO_2 and Al_2O_3 (Table 1), but differs from it by a lower content of CaO and a higher content of Fe_2O_3, MgO, and SO_3.

Table 1. Chemical composition (wt. %) of the HCFA selected from 1–4 fields of the electrostatic precipitator and Portland cement (PC).

HCFA	Components									
	CaO	SiO_2	Al_2O_3	Fe_2O_3	MgO	$\frac{SO_3}{SO_3}$	Na_2O	K_2O	TiO_2	LOI
1	46.15	20.89	4.53	12.65	9.92	3.60	0.75	0.20	0.25	0.60
2	40.6	27.60	4.43	12.06	9.28	3.83	0.80	0.23	0.27	0.60
3	40.0	24.26	6.71	13.45	9.60	3.94	0.72	0.18	0.20	1.0
4	39.69	24.60	7.30	14.29	8.24	2.29	0.71	0.20	0.25	1.96
PC 42.5N	63.99	20.41	4.87	4.18	–	2.46	–	–	–	–
PC [24]	66.4	21.9	5.7	3.2	1.2	0.4	0.7		0.3	–
PC [25]	67.17	22.14	3.12	2.51	–	2.13	–		–	1.68

The major component in the phase composition of fly ashes *1–4* (Table 2) is a predominantly (Ca,Fe)-silicate amorphous phase (19–42 wt %). The clinker phases, such as tricalcium aluminate $3CaO•Al_2O_3$ (9.9–16 wt %) and calcium aluminoferrite $Ca_2Fe_xAl_yO_5$ (13.4–18.7 wt %) are in amounts comparable with the PC clinker. At the same time, the fly ashes do not contain the Ca_3SiO_5 and Ca_2SiO_4 calcium silicate phases, which attain 75–80 wt % in conventional PCs (Table 2) and cause their binding properties. Moreover, the fly ashes contain a considerable amount of free oxides CaO, MgO, SiO_2 as well as the phases of $CaCO_3$ and $CaSO_4$. It should be noted that the content of amorphous phase grows from 19 to 42 wt %, while the content of free CaO decreases from 23.5 to 4.2 wt % in the series of fly ashes from *1* to *4* (Table 2). From a comparison of the chemical and phase composition of the HCFA, it follows that the predominant components of the amorphous phase are (in decreasing order) SiO_2, CaO and Fe_2O_3. It should be noted also that the ratio of SiO_2/CaO in its composition is significantly reduced (from 4.7 to 1.3) in a row of fly ash from 1 to 4. In the calculations of glass composition for the phase of calcium aluminoferrite $Ca_2Fe_x\ Al_yO_5$, x = y = 0.5 was used.

Table 2. Phase composition (wt %) of HCFA selected from 1–4 fields of the electrostatic precipitator and Portland cement (PC).

HCFA	Phases													
	$Ca_3Al_2O_6$	$Ca_2Fe_xAl_yO_5$	CaO	MgO	α - SiO_2	$CaCO_3$	$CaSO_4$	$Ca(OH)_2$	Ca_3SiO_5	Ca_2SiO_4	Ferrospinel	$CaSO_4•0.5H_2O$	$CaSO_4•2H_2O$	Amorphous phase
1	12.7	18.7	23.5	9.3	6.2	–	7.4	–	–	–	3.2	–	–	19.0
2	16.0	13.4	14.6	7.5	9.1	3.9	4.8	–	–	–	2.1	–	–	28.6
3	14.7	13.8	14.0	6.9	6.7	3.0	5.8	–	–	–	2.6	–	–	32.6
4	9.9	16.9	4.2	5.7	5.3	4.9	6.5	2.1	–	–	2.4	–	–	42.1
PC 42.5N	5.8	13.2	–	–	0.5	2.4	–	–	64.5	9.2	–	3.9	0.5	–
PC [24]	7.9	10.1	0.6	0.2	–	–	–	–	66.9	13.2	–	–	–	–
PC [25]	1.2	7.0	–	–	–	1.8	1.4	–	71.1	15.0	–	–	1.2	–

3.2. Compressive Strength of Cured Specimens

As follows from the data presented in Figure 3, the compressive strength (σ_{comp}) of specimens made from 100 % fly ash of the 3rd field at W/T = 0.4 (curve 1) is almost 2 times lower compared to specimens based on fly ash of the 4th field (curve 2). For curve 2, it can be seen that the σ_{comp} value increases from 11 to 22 MPa and then to 30 MPa with the curing age 3, 28 and 80 days, respectively. The fly ashes 3 and 4 (Table 1) have a very similar chemical composition, but significantly differ in particle size (Figure 1). It follows that the higher strength of the samples based on fly ash of the 4th field is presumably due to their higher dispersion (d_{90} < 10 microns), which contributes to an accelerated and more complete interaction of the components of microspheres (especially free CaO and amorphous phase) with the liquid phase to obtain strong structures. Strength tests of samples based on 100 % fly ashes of the 1st and 2nd fields seem to be irrational, since they are characterized by even lower dispersion, higher content of free CaO and, as expected, will have lower strength. It should be noted that the specimens based on fly ash 4 are significantly inferior to the comparison the specimens prepared from PC 42.5N at W/B = 0.4 (Figure 3, curve 3), for which the σ_{comp} value is 25, 48 and 61 MPa at a curing age of 3, 28 and 80 days, respectively.

The high tendency to agglomeration of finely dispersed HCFA does not allow to fully implementing the possibilities of their hydration interaction. The use of high-polymer polycarboxylate superplasticizers prevents

agglomeration, changes the surface properties and promotes the dispersion of micron and submicron particles, leading to the interaction of each individual particle with the liquid phase [16, 17]. The use of 0.12 wt % superplasticizer Melflux 5581F additive allowed reducing the value of W/B to 0.25, while maintaining the necessary fluidity. As a result, high-strength specimens were obtained based on 100 % fly ash of the 4th field (Figure 3, curve 4), the σ_{comp} value of which increases from 24 to 45 and 72 MPa on days 3, 28, and 120, respectively. Thus, the use of finest HCFA in a composition with 0.12 % polycarboxylate superplasticizer Melflux 5581F made it possible to produce specimens with the σ_{comp} value comparable to the strength of specimens based on PC 42.5 N without the addition of superplasticizer. High strength specimens based on HCFA of 4-field of the electrostatic precipitator with the addition of superplasticizer were studied by the CTA and XRD methods in detail. Some of the results of these studies were published in [26].

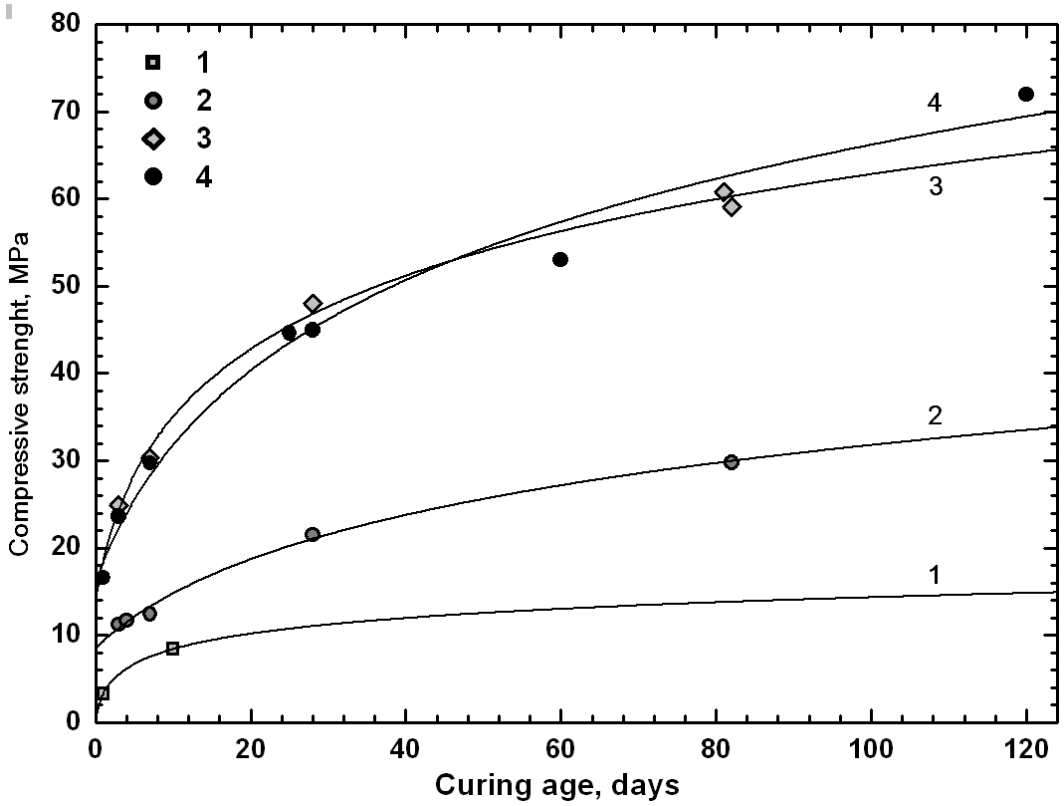

Figure 3. Dependence of the compressive strength on a curing age for the specimens, made at W/B = 0.4 (1 and 2 – from HCFA of 3rd and 4th fields; 3 – from Portland cement 42.5N) and 4 – from HCFA of 4th fields with Melflux 5581F superplactisizer at W/B = 0.25.

3.3. STA analysis of Cured Specimens

From the data in Figure 4a for the specimens after three days of hardening it follows that intensive removal of bound water occurs at temperatures of 60–200 °C, the significantly lower water losses are observed at 200–300 °C. At temperatures of 410–520 °C, characteristic peak of portlandite decomposition by reaction (1) is observed.

$$Ca(OH)_2 = CaO+H_2O. \quad (1)$$

Weight loss at the temperature 520–750 °C is caused by the decomposition of calcium carbonate by the reaction (2):

$$CaCO_3 = CaO + CO_2. \quad (2)$$

With an increase in curing age up to 28 days (Figure 4b), water losses increase in all ranges, but to a greater extent at temperatures of 60–200 °C. The peak of water removal in the range of 320–410 °C also becomes more distinct.

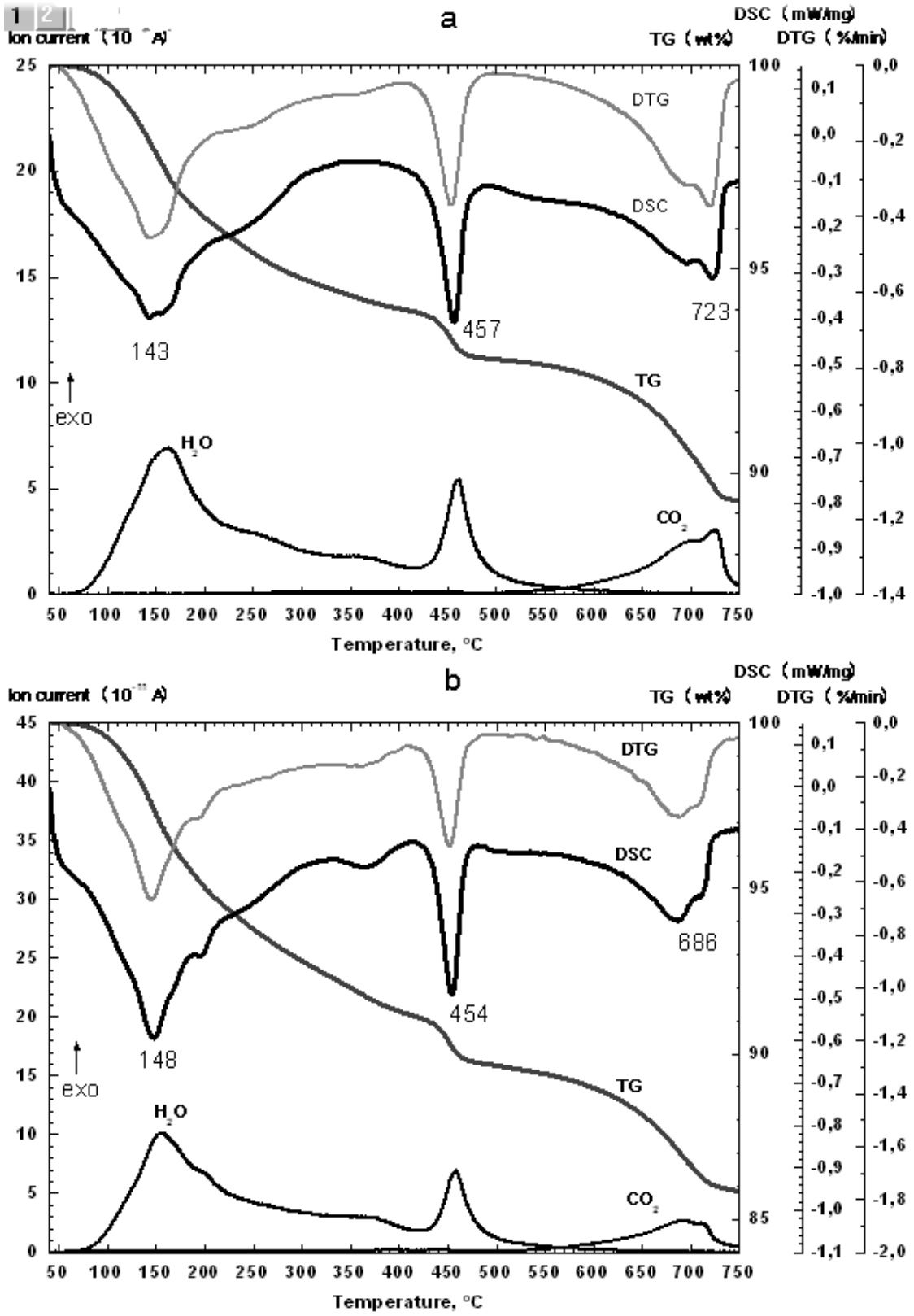

Figure 4. STA data (TG, DTG, DSC and MS of H_2O and CO_2) for the specimens made from HCFA of 4th fields with Melflux 5581F superplactisizer at W/B = 0.25 at a curing age 3 days (a) and 28 days (b).

The data in Table 3 shows that the total loss of bound water Σ (60–410 °C) increases from 5.4 to 12.7 wt % with an increase in the curing age from 1 to 120 days. The greatest contribution to water desorption is observed in the temperature range of 60–200 °C (increasing from 3.6 to 8.1 wt %), and to less extent in the range of 200–320 °C (increasing from 1.35 to 2.9 wt %). In the ranges 320–410 °C and 410–520 °C, the water losses increase during curing age 1–60 days, and decrease at 120 days. The losses of weight due to decarbonization of $CaCO_3$ in the range of 520–750 °C increase for 28-days old specimens, and significantly decrease for the specimens of long-term curing (60 and 120 days).

Table 3. Weight loss (wt %) for the specimens produced from HCFA of 4th field of the electrostatic precipitator at different curing age.

Curing age, days	Temperature range (°C)						
	60–200	200–320	320–410	Σ(60–410)	410–520	520–750	Σ(60–750)
1	3.56	1.35	0.49	5.40	1.16	3.45	10.01
3	3.72	1.68	0.62	6.02	1.24	3.43	10.69
7	3.96	1.71	0.71	6.38	1.33	3.38	11.09
28	4.96	2.56	1.28	8.80	1.65	3.71	14.16
60	7.20	2.79	1.72	11.71	1.99	2.58	16.28
120	8.13	2.90	1.69	12.72	1.41	1.90	16.03

It is known for the systems of similar composition [24, 27], that endothermic peaks in the dehydration range below 200 °C are correlated with the removal of the main part of water from ettringite, as well as from weakly crystallized and amorphous phases of calcium hydrosilicates. According to [24], the maximum intensity at 135–140 °C corresponds to the dehydration of the ettringite, which is actively formed on the first day of Portland cement hydration, and the peak at 115–125 °C corresponds to the dehydration of amorphous (cryptocrystalline) calcium hydrosilicates. Much lower water losses occur in the range of 200–320 °C and correspond to the dehydration of AFm phases and more ordered structures of calcium hydrosilicates [27]. A weak endothermic peak with a water loss in the range of 320–410 °C attributes to the dehydration of poorly crystallized boehmite AlO(OH) or other decomposition products of ettringite, as well as $CaO \cdot Al_2O_3 \cdot 6H_2O$ hydrates [28, 29]. An increase in the amount of $Ca(OH)_2$, which is an indicator of pozzolanic reactions [30, 31], means that its formation during hydration of CaO exceeds its consumption in pozzolanic reactions during 1–60 days of curing, although this trend changes for 120 days of curing.

Thus, the STA study of specimens cured within 1–120 days made it possible to establish the forms of bound water and the tendencies of their change in curing age. It is known that the strength of cement stone grows along with increasing quantity of the hydrated substance [22]. As follows from Table 3, the amount of bound water, which is removed from crystalline hydrates and their thermal decomposition products in the range of 60–410 °C, is increasing from 5.4 to 12.7 wt. % for 1–120 days old specimens and correlates with the strength of the samples changing from 17 to 72 MPa.

3.4. Quantitative Phase Composition of Cured Specimens

The essence of hydraulic binders is to form strong structures of hydrate compounds as a result of their chemical and physicochemical transformations when they interact with water.

As follows from Table 4, only calcium aluminoferrite $Ca_2Fe_xAl_yO_5$ and calcium sulfate $CaSO_4$ crystalline phases completely reacted on the 3rd day of hydration curing. The decrease in the content of CaO phase and the amorphous phase is observed. Ettringite (theoretical composition $3CaO \cdot Al_2O_3 \cdot 3CaSO_4 \cdot 32H_2O$), calcium carbonate $CaCO_3$ and portlandite $Ca(OH)_2$ are actively formed.

On the 28th day of hardening, the main difference is a significant decrease in the amount of calcium carbonate and the formation of poorly crystallized hydrates of calcium carboaluminates $Ca_4Al_2(OH)_{13}(CO_3)_{0.5} \cdot 4H_2O$ and $Ca_4Al_2(OH)_{12}CO_3 \cdot 5H_2O$. In addition, the amount of portlandite significantly increases, but the content of the amorphous phase decreases. On the 120th day of curing, the content of portlandite decreases and the ratio for hydrates of calcium carboaluminates changes, the $Ca_4Al_2(OH)_{12}CO_3 \cdot 5H_2O$ content increases with a simultaneous decrease in $Ca_4Al_2(OH)_{13}(CO_3)_{0.5} \cdot 4H_2O$.

The hydration products of high-calcium fly ashes of Kansk-Achinsk coal [12, 32] contained tricalcium sulfoaluminate (ettringite $3CaO \cdot Al_2O_3 \cdot 3CaSO_4 \cdot 32H_2O$) and monocalcium sulfoaluminate $3CaO \cdot Al_2O_3 \cdot CaSO_4 \cdot 12H_2O$, as well as calcium hydrosilicate gel C-S-H and C-A-S-H. The formation of ettringite and monocalcium sulfoaluminate phases was accompanied by the disappearance of the anhydrite phase and a decrease of the line intensity for the phases CaO, aluminate and calcium aluminoferrite.

From the chemistry of hardening of Portland cements, it is known that ettringite is formed by the interaction of hydrated forms of calcium aluminate $Ca_3Al_2O_6$ and $CaSO_4$ [24]. However, taking into account a small decrease in the $Ca_3Al_2O_6$ content for the 28-days and 120-days old specimens comparing to the initial one, the formation of ettringite during hydration of the HCFA occurs mainly due to the participation of calcium aluminoferrite $Ca_2Fe_xAl_yO_5$. It was also established [24, 30] that the hydration products of calcium aluminoferrite are in many respects similar to the hydration products of $Ca_3Al_2O_6$ aluminate, forming a wide range of solid solutions of hydrates of the type $4CaO (Al_{1-x}, Fe_x)_2O_3 \cdot 19H_2O$ or $3CaO (Al_{1-x},Fe_x)_2O_3 \cdot 6H_2O$. Interacting with $CaSO_4$, they can form almost continuous series of solid solutions of Al, Fe-ettringites.

Table 4. Phase composition (wt %) of the initial HCFA selected from of 4th field of the electrostatic precipitator and the specimens produced from this HCFA at curing age 3, 28 and 120 days.

Phase	Initial HCFA	3 days	28 days [26]	120 days [26]
Crystalline phases				
$Ca_2Fe_xAl_yO_5$	16.9	–	–	–
$Ca_3Al_2O_6$	9.9	11.9	8.1	6.9
$CaSO_4$	6.5	–	–	–
MgO	5.7	6.1	4.0	4.2
α-SiO_2 (quartz)	5.3	5.6	5.7	6.3
$CaCO_3$	4.9	12.6	2.1	3.0
CaO	4.2	3.3	2.3	1.4
Ferrospinel	2.4	2.9	2.7	2.9
$Ca(OH)_2$	2.1	4.0	9.6	8.1
$Ca_6Al_2(SO_4)_3(OH)_{12}\cdot 26H_2O$ (ettringite)	–	8.6	12.4	15.5
Ca_2SiO_4 (larnite)	–	5.7	3.4	4.0
Σ	57.9	60.7	50.3	52.3
Poorly crystallized and amorphous phase				
$Ca_4Al_2(OH)_{13}(CO_3)_{0.5}\bullet 4H_2O$	–	2.0	14.1	5.9
$Ca_4Al_2(OH)_{12}CO_3\bullet 5H_2O$	–	–	5.3	12.7
Amorphous phase	42.1	37.3	30.3	29.1
Σ	42.1	39.3	49.7	47.7

About 21 % and 27 % of the $Ca_2Fe_xAl_yO_5$ phase is consumed on the formation of ettringite according to the data for 28 and 120 days. Under the conditions of sulfate ion deficiency, the significant part of $Ca_2Fe_xAl_yO_5$ is actively involved in the formation of calcium carboaluminate hydrates, which belong to the so-called AFm phases. It is known [24] that hydrates of calcium aluminoferrites in the presence of $Ca(OH)_2$ and $CaSO_4$ can form AFm phases of the general composition $[Ca_2 (Al, Fe) (OH)_6] \bullet X \bullet xH_2O$, where X is one singly charged anion or 0.5 doubly charged anion. The anions X can be OH^-, SO_4^{2-} and CO_3^{2-}. It should be noted that Al- and Fe-substituted AFm phases are isostructural analogues and, depending on temperature, they form solid solutions of various degrees of substitution. In the presence of $Ca(OH)_2$ these phases are weakly crystallized and closely mixed with each other and with other phases, in particular, with the calcium silicate hydrates [24]. Thus, the phases of ettringite and calcium carboaluminate hydrates are solid solutions due to the isomorphic substitution of Al^{3+} for Fe^{3+}. It was not possible to assess the degree of substitution by XRD, mainly due to the low crystallinity of these phases.

The main source of silicates in the HCFA is the amorphous phase of microspheres, which reactivity, as known [8, 24], grows with increasing calcium content. In the initial period, the microspheres having the highest calcium content will participate in the dissolution. Later, as the pH of the solution and the reaction time will increase, the microspheres with lower calcium content and higher silicon content will interact. The result of long hydration time is an increasing amount of calcium hydrosilicates, which usually very weakly crystallize under ordinary conditions. It is also known [24] that during hardening of Portland cement, calcium silicate hydrates are cryptocrystalline substances that serve as a cementing material, linking unhydrated clinker particles and large crystals of $Ca(OH)_2$, ettringite, etc. In the 28-days and 120-days old composite specimens, the amount of the amorphous phase decreased from 42 % to 30 % and 29 % compared to the initial fly ash and, apparently, a significant part is newly formed calcium silicate hydrates, the proportion of which increases with a curing time.

Thus, the high-strength specimens were produced from the finest high-calcium fly ash of the 4th field of the electrostatic precipitator in the composition with the Melflux 5581F superplasticizer at W/B = 0.25. Their compressive strength increased from 17 to 72 MPa as the curing age increased from 1 to 120 days. The strength of these composite specimens is comparable to the strength of specimens based on PC 42.5 N without the addition of superplasticizer. The close mixture of newly formed hydrated phases (ettringite, hydrates of calcium carboaluminates, portlandite and amorphous calcium hydrosilicates) ensures high strength of the material.

4. Conclusion

1. The high-calcium fly ashes (HCFA) selected from each of the 4 fields of the electrostatic precipitator of Krasnoyarsk TPP-2 were studied. It was established that the dispersity and composition of the HCFA vary considerably.

2. Compressive strength tests of the specimens produced from 100 % of the HCFA of the 3rd and the 4th fields at a water/binder ratio of W/B = 0.4 were performed. It was established that the strength of the 4th field specimens is 2 times higher compared to the 3rd field specimens and 2 times lower than the strength PC 42.5N specimens.

3. High-strength specimens were manufactured from the fine high-calcium fly ash of the 4th field (d_{90} < 10 microns) in composition with a polycarboxylate superplasticizer (Melflux 5581F) at a ratio W/B = 0.25. The compressive strength of the specimens increased from 17 to 72 MPa at a curing age from 1 to 120 days. The strength of these specimens is comparable to the strength of specimens based on PC 42.5 without superplasticizer.

4. Synchronous thermal analysis (CTA) and quantitative X-ray phase analysis (XRD) were used to study the phase transformations of the HCFA components in the process of hydration curing, and also to establish the main newly formed hydrate phases providing early and long-term strength. The results on the quantitative phase composition of high-strength specimens create additional opportunities to control the hardening processes of HCFA based binding materials.

5. Acknowledgments

The study was carried out due to the basic research project of the SB RAS V.45.3.3 at Institute of Chemistry and Chemical Technology SB RAS, Federal Research Center «Krasnoyarsk Science Center of the Siberian Branch of the Russian Academy of Sciences».

References

1. Gollakota, A.R.K., Volli, V., Shu, C.M. Progressive utilisation prospects of coal fly ash [Online]: A review. Science of the Total Environment. 2019. 672. Pp. 951–989. DOI: 10.1016/j.scitotenv.2019.03.337. URL: https://doi.org/10.1016/j.scitotenv.2019.03.337
2. Blissett, R.S., Rowson, N.A. A review of the multi-component utilisation of coal fly ash [Online]. Fuel. 2012. 97. Pp. 1–23. DOI: 10.1016/j.fuel.2012.03.024. URL: http://dx.doi.org/10.1016/j.fuel.2012.03.024.
3. Yao, Z.T., Ji, X.S., Sarker, P.K., Tang, J.H., Ge, L.Q., Xia, M.S., Xi, Y.Q. A comprehensive review on the applications of coal fly ash [Online]. Earth-Science Reviews. 2015. 141. Pp. 105–121. DOI: 10.1016/J.EARSCIREV.2014.11.016. URL: https://www.sciencedirect.com/science/article/pii/S0012825214002219?via %3Dihub
4. Belviso, C. State-of-the-art applications of fly ash from coal and biomass: A focus on zeolite synthesis processes and issues [Online]. Progress in Energy and Combustion Science. 2018. 65. Pp. 109–135. DOI: 10.1016/j.pecs.2017.10.004. URL: https://doi.org/10.1016/j.pecs.2017.10.004
5. Sirotyuk, V.V., Lunev, A.A. Strength and deformation characteristics of ash and slag mixture [Online]. Magazine of Civil Engineering. 2017. 74(6). Pp. 1–14. DOI: 10.18720/MCE.74.1. URL: https://elibrary.ru/download/elibrary_30743038_30964333.pdf
6. Lunev, A.A., Sirotyuk, V.V. Stress distribution in ash and slag mixtures [Online]. Magazine of Civil Engineering. 2019. 86(2). Pp. 72–82. DOI: 10.18720/MCE.86.7. URL: https://elibrary.ru/download/elibrary_38582747_15498330.pdf
7. Ovcharenko, G.I., Fomichev, Y.Y. Tehnologia pererabotki visokokalsievoy zoly i shlaka TES v silikatnii kirpich [Processing technology the high calcium ashes and slag from thermal power station in silicate brick]. News of Higher Educational Institutions [Online]. Construction. 2012. (11–12). Pp. 47–53. URL: https://elibrary.ru/item.asp?id=18974275. (rus)
8. Enders, M. Microanalytical characterization (AEM) of glassy spheres and anhydrite from a high-calcium lignite fly ash from Germany [Online]. Cement and Concrete Researc. 1995. 25(6). Pp. 1369–1377. URL: https://doi.org/10.1016/0008-8846(95)00129-Z
9. Sharonova, O.M., Solovyov, L.A., Oreshkina, N.A., Yumashev, V. V, Anshits, A.G. Composition of high-calcium fl y ash middlings selectively sampled from ash collection facility and prospect of their utilization as component of cementing materials [Online]. Fuel Processing Technology. 2010. 91(6). Pp. 573–581. DOI: 10.1016/j.fuproc.2010.01.003. URL: http://dx.doi.org/10.1016/j.fuproc.2010.01.003
10. Zhao, Y., Zhang, J., Tian, C., Li, H., Shao, X., Zheng, C. Mineralogy and chemical composition of high-calcium fly ashes and density fractions from a coal-fired power plant in China. Energy and Fuels. 2010. 24(2). Pp. 834–843. DOI: 10.1021/ef900947y.
11. Sharonova, O.M., Zhizhaev, A.M., Oreshkina, N.A. Composition and structure of calcium aluminosilicate microspheres [Online]. Thermal Engineering. 2017. 64(6). Pp. 415–421. DOI: 10.1134/S0040601517060064. URL: https://elibrary.ru/item.asp?id=31029838
12. Ovcharenko, G.I., Shchukina, Yu.V., Chernyh, K.P. Gazobetony na osnove visokokalsievih zol TEZ [Gas concrete based on high-calcium ash from thermal power station]. Barnaul: Publishing House of Altai State Technical University, 2009 [Online]. URL: https://elibrary.ru/item.asp?id=19629146 (rus)
13. Ahmaruzzaman, M. A review on the utilization of fly ash [Online]. Progress in Energy and Combustion Science. 2010. 36(3). Pp. 327–363. DOI: 10.1016/j.pecs.2009.11.003. URL: http://dx.doi.org/10.1016/j.pecs.2009.11.003.
14. Cross, D., Stephens, J., Vollmer, J. Structural Applications of 100 Percent Fly Ash Concrete. in Proc. 2005 World of Coal Ash (WOCA) Conf., Lexington, KY, USA, Apr. 10–15, 2005 [Online]. URL: http://www.flyash.info/2005/131cro.pdf; 2005. P. 131. URL: https://p2infohouse.org/ref/45/44859.pdf
15. Tumanovskii, A.G. Prospects for the development of coal-steam plants in Russia. Thermal Engineering. 2017. 64(6). Pp. 399–407. DOI: 10.1134/S0040601517060088
16. Li, Z. Advanced concrete technology [Online]. John Wiley & Sons, Inc, New Jersey, USA, 2011. URL: https://epdf.pub/advanced-concrete-technology.html
17. Lange, A., Plank, J. Optimization of comb-shaped polycarboxylate cement dispersants to achieve fast-flowing mortar and concrete [Online]. Journal of Applied Polymer Science. 2015. 132(37). Pp. 1–9. DOI: 10.1002/app.42529
18. Lee, S.H., Kim, K.D., Sakai, E., Daimon, M. Mineralogical variability of fly ashes classified by electrostatic precipitator [Online]. Journal of the Ceramic Society of Japan. 2003. 111(1289). Pp. 11–15. URL: https://doi.org/10.2109/jcersj.111.11
19. Savinkina, M.A., Logvinenko, A.T. Zoli kanskoachinskih burih ugley. (Flu ashes of Kansko-Achinsk brown coals). Novosibirsk: Nauka, 1979.

20. Ovcharenko, G.I. Zoli ugley KATEKa v stroitel'nih materialah (KATEK coal ashes in building materials). Krasnoyarsk: Publishing House Krasnoyarsk. univ., 1992.
21. Solovyov, L.A. Full-profile refinement by derivative difference minimization research papers. Journal of Applied Crystallography. 2004. 37(5). Pp. 743–749. DOI: 10.1107/S0021889804015638.
22. Sharonova, O.M., Anshits, N.N., Solovyov, L.A., Salanov, A.N., Anshits, A.G. Relationship between composition and structure of globules in narrow fractions of ferrospheres [Online]. Fuel. 2013. 111. Pp. 332–343. DOI: 10.1016/j.fuel.2013.03.059. URL: http://dx.doi.org/10.1016/j.fuel.2013.03.059.
23. Yamada, K., Takahashi, T., Hanehara, S., Matsuhisa, M. Effects of the chemical structure on the properties of polycarboxylate-type superplasticizer [Online]. Cement and Concrete Research. 2000. 30(2). Pp. 197–207. URL: http://doi.org/10.1016/S0008-8846(99)00230-6.
24. Taylor, H.F.W. Cement Chemistry. 2nd Ed Thomas Telford [Online]. London, 1997. 476 p. URL: https://www.icevirtuallibrary.com/doi/book/10.1680/cc.259
25. Sorelli, L., Constantinides, G., Ulm, F.J., Toutlemonde, F. The nano-mechanical signature of Ultra High Performance Concrete by statistical nanoindentation techniques. Cement and Concrete Research. 2008. 38(12). Pp. 1447–1456. DOI: 10.1016/j.cemconres.2008.09.002.
26. Sharonova, O.M., Kirilets, V.M., Yumashev, V.V., Solovyov, L.A., Anshits, A.G. Phase composition of high strength binding material based on fine microspherical high-calcium fly ash [Online]. Construction and Building Materials. 2019. 216. Pp. 525–530. DOI: 10.1016/j.conbuildmat.2019.04.201. URL: https://doi.org/10.1016/j.conbuildmat.2019.04.201.
27. Deschner, F., Winnefeld, F., Lothenbach, B., Seufert, S., Schwesig, P., Dittrich, S., Goetz-Neunhoeffer, F., Neubauer, J. Hydration of Portland cement with high replacement by siliceous fly ash [Online]. Cement and Concrete Research. 2012. 42(10). Pp. 1389–1400. DOI: 10.1016/j.cemconres.2012.06.009. URL: http://dx.doi.org/10.1016/j.cemconres.2012.06.009
28. Panasyuk, G.P., Belan, V.N., Voroshilov, I.L., Kozerozhets, I.V. Hydrargillite → boehmite transformation. Inorganic Materials. 2010. 46(7). Pp. 747–753. DOI: 10.1134/S0020168510070113.
29. Torréns-Martín, D., Fernández-Carrasco, L., Blanco-Varela, M.T. Thermal analysis of blended cements. Journal of Thermal Analysis and Calorimetry. 2015. 121(3). Pp. 1197–1204. DOI: 10.1007/s10973-015-4569-1.
30. Giergiczny, Z. The hydraulic activity of high calcium fly ash. Journal of Thermal Analysis and Calorimetry. 2006. 83(1). Pp. 227–232. DOI: 10.1007/s10973-005-6970-7.
31. Roszczynialski, W. Determination of pozzolanic activity of materials by thermal analysis. Journal of Thermal Analysis and Calorimetry. 2002. 70(2). Pp. 387–392. DOI: 10.1023/A:1021660020674.
32. Ovcharenko, G.I., Shchukina, Yu.V., Khizhinkova, E.Yu. Analiz productov gidratazii zol uglei KATEKa metodami DTA i DSK [Analysis of hydration products for coal ashes of KATEK coals by DTA and DSC methods] [Online]. Polzunovsky vestnik. 2006. 2. Pp. 210–212. URL: https://elibrary.ru/item.asp?id=13027758

Contacts:

Olga Sharonova, +7(923)3697036; sharon05@yandex.ru
Vladimir Yumashev, +7(962)0780323; yumashev_vlad@mail.ru
Leonid Solovyov, +7(906)9732912; leosol@icct.ru
Alexander Anshits, +7(950)4370735; anshits@icct.ru

Инженерно-строительный журнал

ISSN 2071-0305

сайт журнала: http://engstroy.spbstu.ru/

DOI: 10.18720/MCE.91.6

Тонкодисперсная высококальциевая летучая зола как основа композитного цементирующего материала

О.М. Шаронова*, В.В. Юмашев, Л.А. Соловьев, А.Г. Аншиц

Федеральное государственное бюджетное научное учреждение «Федеральный исследовательский центр «Красноярский научный центр Сибирского отделения Российской академии наук», г. Красноярск, Россия

** E–mail: sharon05@yandex.ru*

Ключевые слова: высококальциевая летучая зола, цементирующие материалы, суперпластификатор, гидратация, прочность на сжатие, соединения кальция, рентгенофазовый анализ

Аннотация. Исследованы высококальциевые летучие золы (ВКЛЗ), отобранные с каждого из 4-х полей электрофильтров (ЭФ) Красноярской ТЭЦ-2. Определено, что распределение по размерам, химический и количественный фазовый состав значительно изменяются от 1 к 4 полю ЭФ. Образцы высокой прочности были получены на основе тонкодисперсной ВКЛЗ с 4 поля ЭФ (d_{90} < 10 микрон) в композиции с суперпластификатором при соотношении вода:связующее B/C = 0.25, их прочность на сжатие возрастала от 17 до 72 МПа при отверждении от 1 до 120 суток. Прочность этих образцов сопоставима с прочностью образцов на основе портландцемента ПЦ 42.5Н без добавки суперпластификатора. Образцы высокой прочности исследованы методами синхронного термического анализа (СТА) и количественного рентгенофазового анализа (РФА). Установлено, что главными новообразованными фазами являются эттрингит $3CaO•Al_2O_3•3CaSO_4•32H_2O$, а также гидраты карбоалюминатов кальция $Ca_4Al_2(OH)_{13}(CO_3)0{,}5•4H_2O$ и $Ca_4Al_2(OH)_{12}CO_3•5H_2O$ с низкой окристаллизованностью. За счет замещения Al^{3+} на Fe^{3+} новые фазы могут образовывать широкие ряды твердых растворов. Из совокупности данных методов СТА и РФА можно утверждать, что при увеличении сроков твердения возрастает вклад превращений кальцийсиликатного аморфного вещества с образованием скрытокристаллических гидросиликатов кальция, повышающих начальную и долговременную прочность материала. Фазовые превращения и показатели прочности позволяют использовать тонкодисперсные высококальциевые летучие золы угольных ТЭЦ как самостоятельный цементирующий материал в современных технологиях получения строительных материалов, в частности, в технологии самоуплотняющихся композитных бетонов (СУБ). Предложенная альтернатива цементу способствует решению комплексной экологической проблемы: (1) в области теплоэнергетики уменьшается накопление тонкодисперсных частиц золы, а, следовательно, уменьшается загрязнение вод, почв и атмосферы тонкими пылевидными частицами и (2) часть цемента в промышленности строительных материалов замещается на ВКЛЗ, что позволит сэкономить энерго- и природные ресурсы.

Литература

1. Gollakota A.R.K., Volli V., Shu C.M. Progressive utilisation prospects of coal fly ash: A review // Science of the Total Environment. 2019. (672). Pp. 951–989. DOI: 10.1016/j.scitotenv.2019.03.337.
2. Blissett R.S., Rowson N.A. A review of the multi-component utilisation of coal fly ash // Fuel. 2012. (97). Pp. 1–23. DOI: 10.1016/j.fuel.2012.03.024.
3. Yao Z.T., Ji X.S., Sarker P.K., Tang J.H., Ge L.Q., Xia M.S., Xi Y.Q. A comprehensive review on the applications of coal fly ash // Earth-Science Reviews. 2015. (141). Pp. 105–121. DOI: 10.1016/J.EARSCIREV.2014.11.016.
4. Belviso C. State-of-the-art applications of fly ash from coal and biomass: A focus on zeolite synthesis processes and issues // Progress in Energy and Combustion Science. 2018. (65). Pp. 109–135. DOI: 10.1016/j.pecs.2017.10.004.
5. Sirotyuk V.V., Lunev A.A. Strength and deformation characteristics of ash and slag mixture // Magazine of Civil Engineering. 2017. 6(74). Pp. 1–14. DOI: 10.18720/MCE.74.1.
6. Lunev A.A., Sirotyuk V.V. Stress distribution in ash and slag mixtures // Magazine of Civil Engineering. 2019. 2(86). Pp. 72–82. DOI: 10.18720/MCE.86.7.
7. Овчаренко Г.И. Фомичев Ю.Ю. Технология переработки высококальциевой золы и шлака тэц в силикатный кирпич [Электронный ресурс] // Известия высших учебных заведений. Строительство. 2012. № 11–12. С. 47–53. URL: https://elibrary.ru/item.asp?id=18974275

8. Enders M. Microanalytical characterization (AEM) of glassy spheres and anhydrite from a high-calcium lignite fly ash from Germany [Электронный ресурс] // Cement and Concrete Researc. 1995. 6(25). Pp. 1369–1377. URL: https://doi.org/10.1016/0008-8846(95)00129-Z
9. Sharonova O.M., Solovyov L.A., Oreshkina N.A., Yumashev V. V, Anshits A.G. Composition of high-calcium fl y ash middlings selectively sampled from ash collection facility and prospect of their utilization as component of cementing materials // Fuel Processing Technology. 2010. 6(91). Pp. 573–581. DOI: 10.1016/j.fuproc.2010.01.003.
10. Zhao Y., Zhang J., Tian C., Li H., Shao X., Zheng C. Mineralogy and chemical composition of high-calcium fly ashes and density fractions from a coal-fired power plant in China // Energy and Fuels. 2010. 2(24). Pp. 834–843. DOI: 10.1021/ef900947y.
11. Шаронова О.М., Орешкина Н.А. Жижаев А.М. Состав и строение кальцийалюмосиликатных микросфер // Теплоэнергетика. 2017. 6(64). С. 22–29. DOI: 10.1134/S0040363617060066.
12. Овчаренко Г.И., Щукина Ю.В., Черных К.П. Газобетоны на основе высококальциевых зол ТЭЦ [Электронный ресурс]. Барнаул: Изд-во АлтГТУ, 2009. 233 с. URL: https://elibrary.ru/item.asp?id=19629146
13. Ahmaruzzaman M. A review on the utilization of fly ash // Progress in Energy and Combustion Science. 2010. 3(36). Pp. 327–363. DOI: 10.1016/j.pecs.2009.11.003.
14. Cross D., Stephens J., Vollmer J. Structural Applications of 100 Percent Fly Ash Concrete [Электронный ресурс] // in Proc. 2005 World of Coal Ash (WOCA) Conf., Lexington, KY, USA, Apr. 10–15, 2005. P 131. URL: http://www.flyash. info/2005/131cro.pdf
15. Тумановский А.Г. Перспективы развития угольных ТЭС России // Теплоэнергетика. 2017. 6(64). С. 3–13. DOI: 10.1134/S004036361706008X.
16. Li. Z. Advanced concrete technology [Электронный ресурс]. John Wiley & Sons, Inc, New Jersey, USA, 2011. 506 p. URL: https://epdf.pub/advanced-concrete-technology.html
17. Lange A., Plank J. Optimization of comb-shaped polycarboxylate cement dispersants to achieve fast-flowing mortar and concrete // Journal of Applied Polymer Science. 2015. 37(132). Pp. 1–9. DOI: 10.1002/app.42529.
18. Lee S.H., Kim K.D., Sakai E., Daimon M. Mineralogical variability of fly ashes classified by electrostatic precipitator [Электронный ресурс] // Journal of the Ceramic Society of Japan. 2003. 1289(111). Pp. 11–15. URL: https://doi.org/10.2109/jcersj.111.11
19. Савинкина М.А., Логвиненко А.Т. Золы канско-ачинских бурых углей. Новосибирск: Наука, 1979. 168 с.
20. Овчаренко Г.И. Золы углей КАТЭКа в строительных материалах. Краснодар: Изд-во Краснояр. ун-та, 1992. 216 с.
21. Solovyov L.A. Full-profile refinement by derivative difference minimization research papers // Journal of Applied Crystallography. 2004. 5(37). Pp. 743–749. DOI: 10.1107/S0021889804015638.
22. Sharonova O.M., Anshits N.N., Solovyov L.A., Salanov A.N., Anshits A.G. Relationship between composition and structure of globules in narrow fractions of ferrospheres // Fuel. 2013. (111). Pp. 332–343. DOI: 10.1016/j.fuel.2013.03.059.
23. Yamada K., Takahashi T., Hanehara S., Matsuhisa M. Effects of the chemical structure on the properties of polycarboxylate-type superplasticizer [Электронный ресурс] // Cement and Concrete Research. 2000. 2(30). Pp. 197–207. URL: http://doi.org/10.1016/S0008-8846(99)00230-6
24. Taylor H.F.W. Cement Chemistry. 2nd Ed. Thomas Telford [Электронный ресурс]. London, 1997. 476 p. URL: https://www.icevirtuallibrary.com/doi/book/10.1680/cc.259
25. Sorelli L., Constantinides G., Ulm F.J., Toutlemonde F. The nano-mechanical signature of ultra high performance concrete by statistical nanoindentation techniques // Cement and Concrete Research. 2008. 12(38). Pp. 1447–1456. DOI: 10.1016/j.cemconres.2008.09.002.
26. Sharonova O.M., Kirilets V.M., Yumashev V. V, Solovyov L.A., Anshits A.G. Phase composition of high strength binding material based on fine microspherical high-calcium fly ash // Construction and Building Materials. 2019. (216). Pp. 525–530. DOI: 10.1016/j.conbuildmat.2019.04.201.
27. Deschner F., Winnefeld F., Lothenbach B., Seufert S., Schwesig P., Dittrich S., Goetz-Neunhoeffer F., Neubauer J. Hydration of Portland cement with high replacement by siliceous fly ash // Cement and Concrete Research. 2012. 10(42). Pp. 1389–1400. DOI: 10.1016/j.cemconres.2012.06.009.
28. Панасюк Г.П., Белан В.Н., Ворошилов И.Л., Козерожец И.В. Превращение гидраргиллит → бемит [Электронный ресурс] // Неорганические материалы. 2010. № 7(46). С. 831–837. URL: https://elibrary.ru/download/elibrary_15108829_49939095.pdf
29. Torréns-Martín D., Fernández-Carrasco L., Blanco-Varela M.T. Thermal analysis of blended cements // Journal of Thermal Analysis and Calorimetry. 2015. 3(121). Pp. 1197–1204. DOI: 10.1007/s10973-015-4569-1.
30. Giergiczny Z. Effect of some additives on the reactions in fly ash-Ca(OH)2 system // Journal of Thermal Analysis and Calorimetry. 2004. 3(76). Pp. 747–754. DOI: 10.1023/B:JTAN.0000032259.80031.b2.
31. Roszczynialski W. Determination of pozzolanic activity of materials by thermal analysis // Journal of Thermal Analysis and Calorimetry. 2002. 2(70). Pp. 387–392. DOI: 10.1023/A:1021660020674.
32. Овчаренко Г.И., Щукина Ю.В., Хижинкова Е.Ю. Анализ продуктов гидратации зол углей катэка методами ДТА и ДСК [Электронный ресурс] // Позуновский вестник. 2006. № 2. С. 210–212. URL: https://elibrary.ru/item.asp?id=13027758

Контактные данные:

Ольга Михайловна Шаронова, +7(923)3697036; эл. почта: sharon05@yandex.ru

Владимир Витальевич Юмашев, +7(962)0780323; эл. почта: yumashev_vlad@mail.ru

Леонид Александрович Соловьев, +7(906)9732912; эл. почта: leosol@icct.ru

Александр Георгиевич Аншиц, +7(950)4370735; эл. почта: anshits@icct.ru